IHJPAS. 37 (1) 2024
Ibn Al-Haitham Journal for Pure and Applied Sciences
Journal homepage: jih.uobaghdad.edu.iq
PISSN: 1609-4042, EISSN: 2521-3407

Anti-Oxidant and Anti-Microbial Activities of [ZnO: CoO/ Eugenol] and [ZnO: Fe_2O_3/ Eugenol] Nanocomposites

[1]Fatin Ahmed Al-Jubouri* **[2]Basim Ibrahim Al-Abdaly**
[1,2] Department of Chemistry/ College of Sciences, University of Baghdad, Baghdad, Iraq.

*Corresponding Author: faten.ahmed1205m@sc.uobaghdad.edu.iq

Received 22 January 2023, Received 12 March 2023, Accepted 20 March 2023, Published 20 January 2024

doi.org/10.30526/37.1.3233

Abstract

Metal oxide nanocomposites (MONCs) manufacturing is increasingly gaining popularity. The primary cause of this is the broad range of applications for such materials, which include fuel cells, photovoltaics, cosmetics, medicine, semiconductor packing materials, water treatment, and catalysts. Due to their size, stability, high surface area, catalytic activity, simplicity in fabrication, and selectivity for particular reactions. The MONCs with various morphologies have been created by physical, chemical, and biological processes, such as sol-gel, hydrothermal, co-precipitation, solvothermal, and microwave irradiation. Eugenol (4-allyl-2-methoxyphenol) is a major component of clove essential oil and it was found in various plant groups, has been widely utilized, and famously stated to have a variety of important biological activities. It is a good starting material for the synthesis of a wide variety of derivatives with different activity. Due to the presence of many functional groups in its structure, including allyl ($-CH_2-CH=CH_2$), phenol (-OH), and methoxy ($-OCH_3$). The eugenol was taken with metal oxides (zinc cobalt oxides ZnO: CoO) to synthesis [ZnO: CoO/ Eug] and (zinc ferric oxides ZnO: Fe_2O_3) to synthesis [ZnO: Fe_2O_3/ Eug] as nanocomposites by hydrothermal method and characterization the compounds using: (FT-IR, AFM, SEM, EDX, XRD) techniques. Then, they tested their biological activities through antimicrobial and antioxidant.

Keywords: Anti-microbial, Anti-oxidant, Eugenol, Hydrothermal method, Metal oxides nanocomposites.

1. Introduction

Nano is a Greek prefix that signifies midget; the terms technology and the Greek numerical prefix nano, which means one billionth, are combined to form the phrase nanotechnology. As a result, nanotechnology or nanoscaled technology is commonly considered to be at a size below 0.1 μm or 100 nm (a nanometer is one billionth of a meter, 10^{-9} m). Nanotechnology, often abbreviated as nanotech, is the science of manipulating matter at the atomic and molecular levels [1] or can be defined as the physical and biological processes performed to handle material to create materials with unique properties for use in various applications [2].

Nanocomposite materials (NCMs) are composites with more than one solid phase with at least one dimension in the nanometer range (1-100) nm. The solid phases can be mixtures of amorphous, semicrystalline, and crystalline states. They can have any composition and be organic, inorganic, or even both [3]. The potential of nanocomposites, a high-performance material that displays unexpected property combinations and unique design options, is so outstanding that it is helpful in a wide range of applications [4], such as medical treatments, civil, health, fabrication, information, techniques, environments, and energy sources [5]. Synthesis of metal oxide nanocomposite (MONCs): the synthesis of uniform-size nanocomposite is critical because its properties include optical, magnetic, electrical, and biological properties depending on their size and dimensions, more than one method can be used to synthesize the metal oxides (nanoparticles and nanocomposite) [6], and this study utilized a hydrothermal preparation approach since it needs low temperature, cheap costs, and a short time while being ecologically clean and nontoxic, with key parameters that can be readily modified and controlled [7]. The hydrothermal method can be defined as any heterogeneous reaction with solvents or water minerals under high temperature and pressure conditions to dissolve relatively insoluble materials under normal conditions [8].

Eugenol (EUG), also known as 4-allyl-2-methoxyphenol, is a phenylpropanoid with a substituted allyl chain for guaiacol [9]. The name is taken from Eugenia aromaticum, also known as Eugenia caryophyllata, which is the scientific name for clove [10], and it's traditionally produced from the dried flower buds of Eugenia caryophyllata Thunb (Myrtaceae) [11]. Also, it is a naturally occurring compound found in various plant groups [9]. It is a transparent to light yellow greasy liquid. It is the primary component of clove essential oil [10]; it makes up about 83–95 percent of clove oil [12]. It's the most volatile, biologically active component, giving cloves their characteristic scent [10,11]. It has a low chemical stability, is susceptible to oxidation, and is soluble in tiny amounts in water but readily dissolves in organic solvents [13]. The EUG is an antimicrobial phenolic component of cinnamon essential oil. It is well-known for its anti-inflammatory, antioxidant, anticarcinogenic, anti-virus, anti-bacteria, anti-coagulation, anti-platelet aggregation, and analgesic properties [14,15] due to the presence of many functional groups, including allyl ($-CH_2-CH=CH_2$), methoxy (OCH_3), and phenol (OH) [16] Figure 1. This work is to study the effects of [metals oxides/ eugenol] nanocomposites on biological applications through antimicrobial and antioxidant activities after being synthesized by hydrothermal method.

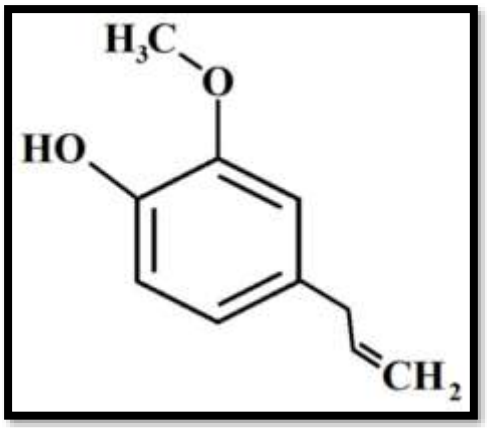

Figure 1. Chemical structure of eugenol [13]

2. Materials and Methods

The organic compounds used in the present research had the most excellent purity possible. Different apparatuses were used in this work to characterize the synthesized nanostructures, as illustrated briefly below in **Table 1.**

Table 1. Instruments utilized in this current project

Model AA3000/ Angstrom Advanced Inc. USA	Chemistry Analysis Center/ Baghdad	Morphology of coated surfaces
TESCAN-MIRA3 Czech Repblic	University of Tabriz/ Iran	Morphology of coated surfaces
ADX 2700 Angstrom Advanced Inc. USA	University of Kashan/ Iran	Crystals structure & Type of phase
SHIMADZU FT-IR 8400S/Japan	Chemistry department, college of science, University of Baghdad	Chemical Compounds

2.1 Synthesis of [metal oxides/ eugenol] nanocomposites by hydrothermal method:

2.1.1 Synthesis of [ZnO: CoO / Eug] nanocomposite

Two salts were used; the first one was $Zn(CH_3CO_2)_2$ (2.29 g, 0.5 M), which dissolved in 25 mL of deionized water to form the first solution, the second salt was $Co(CH_3CO_2)_2.4H_2O$ (3.114 g, 0.5 M) which dissolved in 25 mL of deionized water to form the second solution, then mix the solutions (1) and (2), and add to them (1 mL) of eugenol, and the last addition for the mixture was 4 ml of sodium hydroxide (NaOH) (0.5 g, 0.5 M) after dissolved it with 25 mL of deionized water, the mixture was taken and placed in the Teflon liner autoclave cell, and heated at (150 °C) for one hour with (heating rate = 2 °C /min). The cell was cooled, and the mixture was separated by centrifugation at 4000 (rpm) for 15 minutes. After that, the separated sample was dried in an oven at (75 °C).

2.1.2 Synthesis of [ZnO: Fe_2O_3 / Eug] nanocomposite

It was carried out by the same method used and mentioned in the paragraph above, taking into consideration some of the variables needed for the synthesis, like using Ferric (III) chloride $FeCl_3$ (2.027 g, 0.5 M) instead of Co $(CH_3CO_2)_2.4H_2O$ (3.114 g, 0.5 M).

3. Results and Discussion

3.1 Atomic force microscopy (AFM)

Surface morphology and roughness for the [ZnO: CoO /Eug] nanocomposite prepared by the hydrothermal method were indicated in the AFM images in **Table 2** and **Figure 2**. The results confirm that the average roughness (Ra) was 4.39 nm, and the mean standard deviation (Rq) was 6.72 nm. The mean diameter distribution of particle size generated from the analysis of the nanocomposite shows particle sizes ranging from 80 to 90 nm. While the results of the [ZnO: Fe_2O_3 /Eug] nanocomposite sample indicates a decrease in the surface roughness to 6.95 nm, with a root mean square deviation of 9.48 nm, as shown in **Figure 3**. The mean diameter distribution of nanoparticles in the diagram shows that particle sizes range from less than 60 to 80 nm.

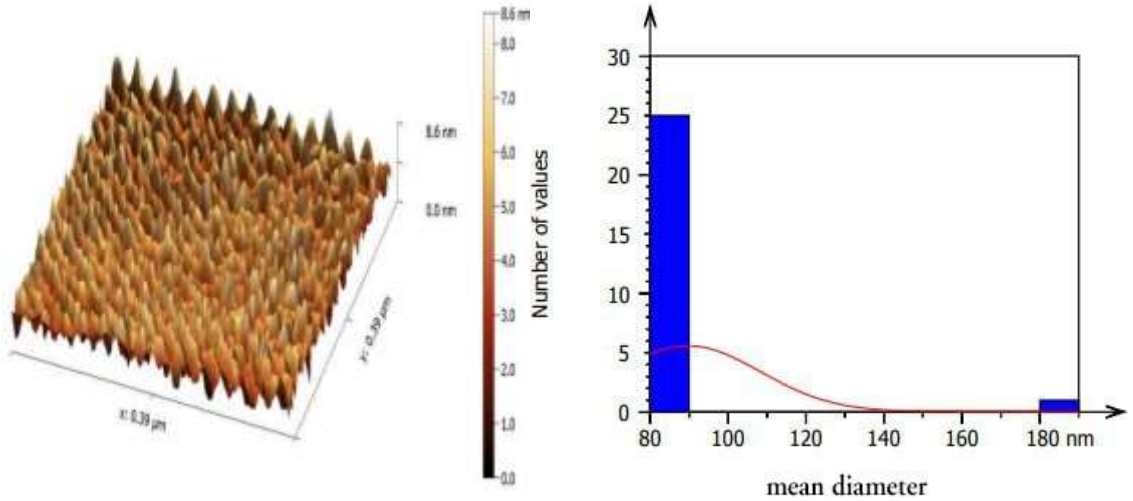

Figure 2. AFM analysis image and particle size distribution of the [ZnO: CoO / Eug] nanocomposite

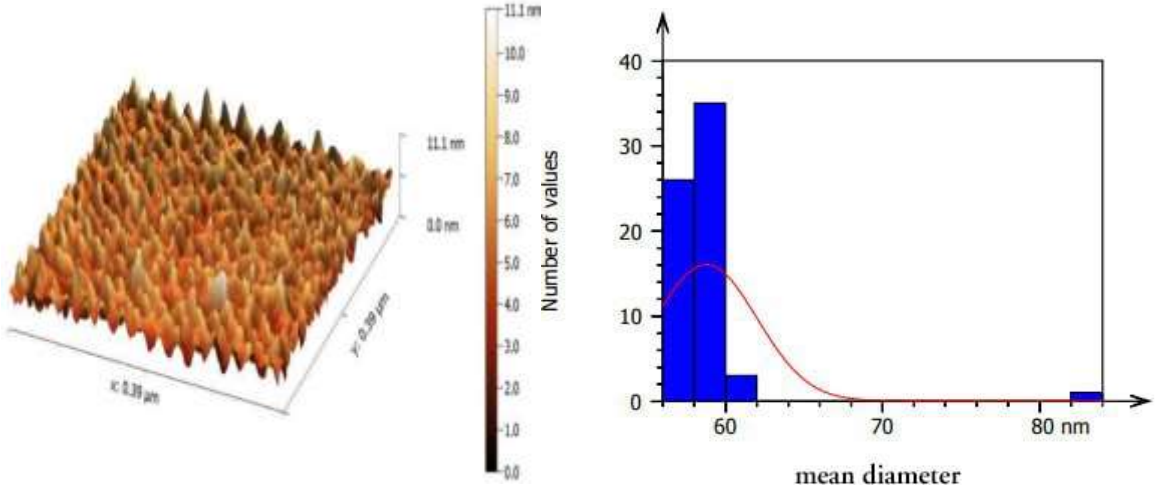

Figure 3. The AFM analysis image and particle size distribution of the [ZnO: Fe_2O_3/ Eug] nanocomposite

Table 2. Estimated data from AFM measurements of nanocomposites

Conditions	Ra (nm)	Rq (nm)	Mean diameter (nm)
[ZnO: CoO/ Eug]	4.39	6.72	89.62
[ZnO: Fe_2O_3 / Eug]	6.95	9.48	58.77

3.2 Scanning Electron Microscopy and Energy Dispersive X–ray (SEM/EDX)

Figure 4 (A, B) illustrates the SEM image of [ZnO: CoO/ Eug] prepared by hydrothermal method's. At various magnifications, this image reveals the topography of the surface stacked sheets among themselves and suggests the role played by the eugenol material used during preparation as well as the type of preparation method, which causes the materials to adhere to one another when heated [17]. The shape of [ZnO: CoO/ Eug] is nanosheets. **Figure 5** explains the EDX analysis and displays the elemental percentages; as a result, it assumes that this crucial examination provides information on the materials' purity, as indicated by the percentage of Zn, which was around 18.57%, 25.64% of Co, 32.55% of oxygen, and another percentage 23.25% return to the carbon of eugenol.

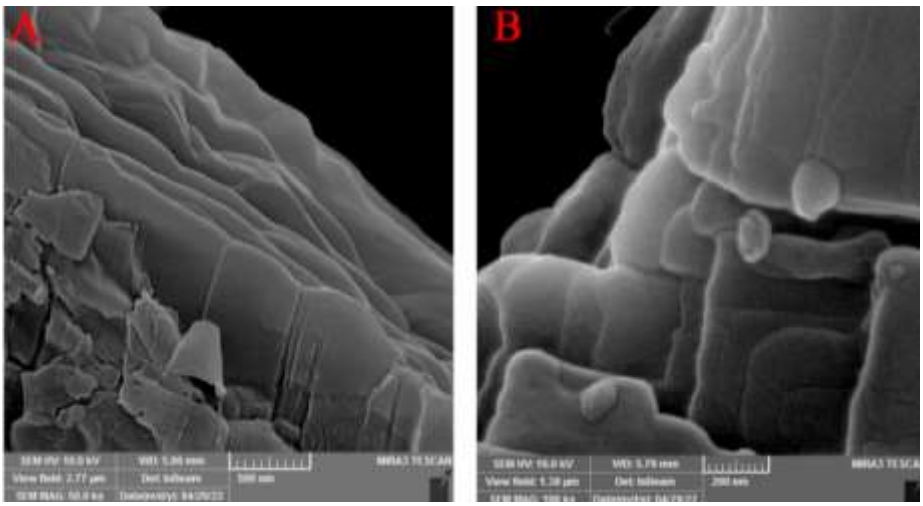

Figure 4. The SEM Images (A, B) of [ZnO: CoO/ Eug] with different magnifications 50Kx, 100 Kx, respectively

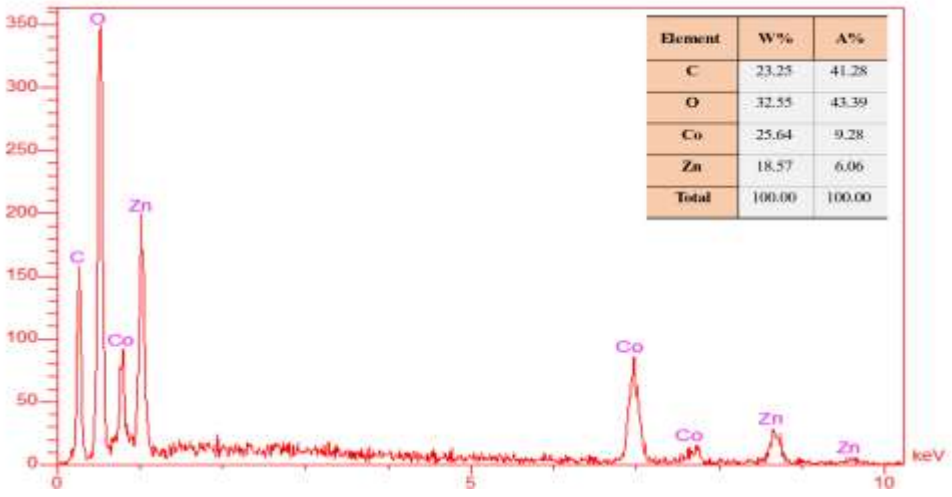

Figure 5. The EDX analysis for [ZnO: CoO/ Eug] nanocomposite

Figure 6 (A, B) shows the SEM images of [ZnO: Fe_2O_3/ Eug] and the general shape of the morphology of [ZnO: Fe_2O_3/ Eug] displaying with different magnifications. Tiny particles of nanomaterials are clearly shown aggregating with each other [18]. The shape of [ZnO: Fe_2O_3/ Eug] is nanoparticles**. Figure 7** explains the EDX result of [ZnO: Fe_2O_3/ Eug]; therefore, all of the compound materials have shown different percentage.

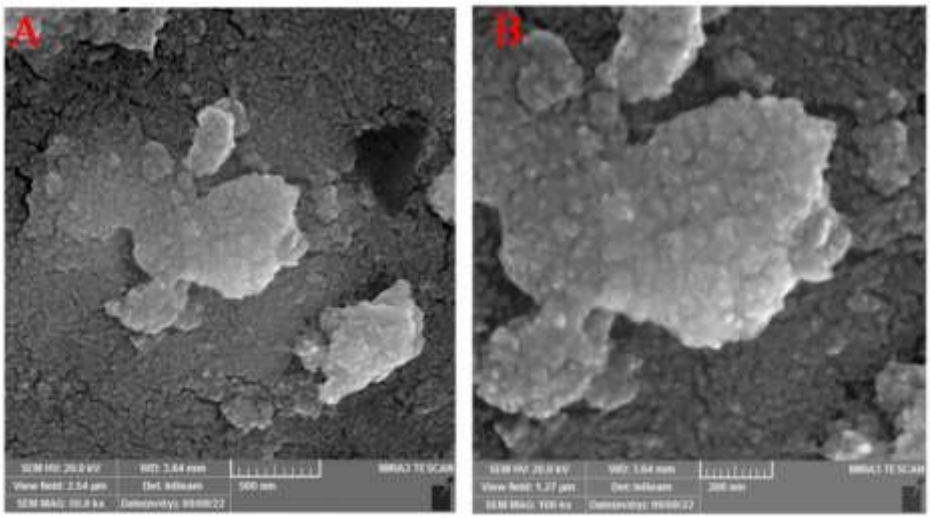

Figure 6. The SEM Images (A, B) of [ZnO: Fe_2O_3/ Eug] with different magnifications 50Kx, 100 Kx, respectively

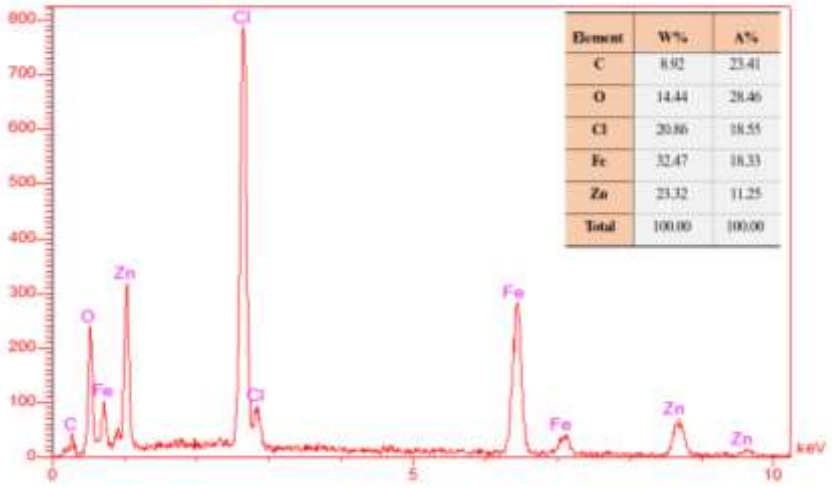

Figure 7. The EDX analysis for [ZnO: Fe_2O_3/ Eug] nanocomposite

3.3 The X–ray diffraction (XRD)

Figure 8 shows the pattern of [ZnO: CoO/ Eug], as shown there are some peaks in agreement with the Zn and Co_3O_4 according to JCPDS 00-001-1238 for Zn [19], while JCPDS 01-080-1545 below to Co3O4 [20]. The average crystallite size of [ZnO: CoO/ Eug] was about 59.01 nm, and the other peaks returned to the carbons atom. The FWHM and Crystallite size of [ZnO: CoO/ Eug] are shown in **Table 3**. The nanoparticles' crystallite size was calculated using Debye Scherrer's formula [21]. **Figure 9** shows the pattern of [ZnO: Fe_2O_3/ Eug]; there was more crystallinity of ZnO- Fe_2O_3 and different intensities of diffraction peaks [18], which matched with 01-080-0075 [22] and 01-084-0311 [23]. From **Table 4**, it can be concluded that the diffraction angles return to Fe_2O_3 and ZnO as individual elements. The average crystallite size was 23.8 nm, calculated using Debye Scherrer's formula [21].

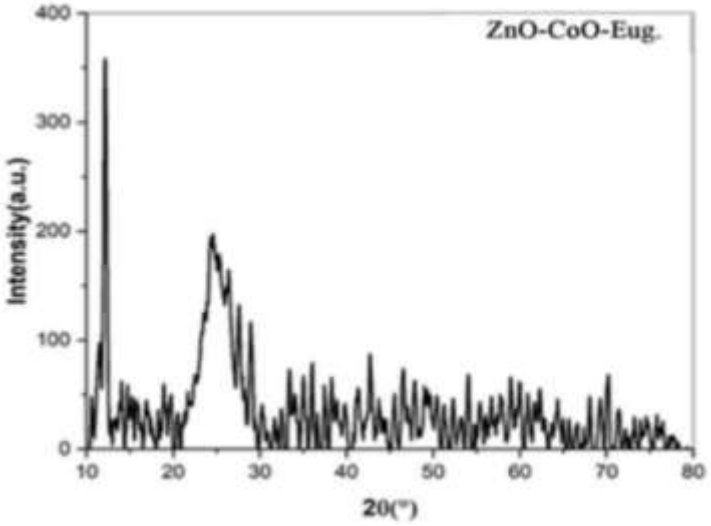

Figure 8. The XRD pattern of [ZnO: CoO/ Eug] nanocomposite

Table 3. The FWHM and Crystallite size of [ZnO: CoO/ Eug] nanocomposite

Nanocomposite	The highest peaks refer	2 theta (degree)	d-spacing [Å]	FWHM (deg)	2 theta (Rad.)	FWHM (Rad.)	D (nm)	Matched by
[ZnO: CoO/ Eug]	Zn	71.2564	1.32235	0.48	1.244	0.008	51.486	00-001-1238
	Co_3O_4	38.2588	2.35255	0.148	0.668	0.003	68.518	01-080-1545
		69.2846	1.35621	0.394	1.209	0.007	57.038	

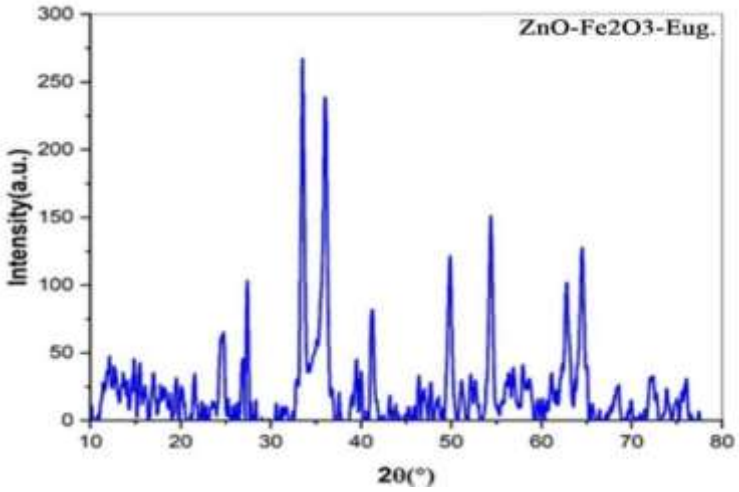

Figure 9. The XRD pattern of [ZnO: Fe_2O_3/ Eug] nanocomposite

Table 4. The FWHM and Crystallite size of [ZnO: Fe_2O_3/ Eug] nanocomposite

Nanocomposite	The highest peaks refer	2 theta (degree)	d-spacing [Å]	FWHM (deg)	2 theta (Rad.)	FWHM (Rad.)	D (nm)	Matched by
[ZnO: Fe_2O_3/ Eug]	Fe_2O_3	24.7279	3.60048	0.590	0.432	0.010	14.808	01-084-0311
		33.5328	2.67250	0.394	0.585	0.007	24.204	01-084-0311
	ZnO-Fe_2O_3	36.0977	2.48828	0.394	0.630	0.007	24.970	01-080-0075; 01-084-0311
	Fe_2O_3	41.2738	2.18740	0.590	0.720	0.010	17.897	01-084-0311
		49.8721	1.82857	0.590	0.870	0.010	20.870	01-084-0311
		54.4059	1.68642	0.492	0.950	0.009	27.731	01-084-0311
	ZnO-Fe_2O_3	62.8537	1.47856	0.787	1.097	0.014	22.110	01-080-0075; 01-084-0311
	Fe_2O_3	64.5143	1.44326	0.480	1.126	0.008	38.449	01-084-0311

3.4 Fourier transform infrared spectroscopy analysis (FT-IR)

The FTIR spectrum of [ZnO: CoO/ Eug], Figure 10 revealed a peak at 578 cm^{-1} that was assigned to stretching vibration of (Zn-O) bond [24] and the broad absorption band at 3444 cm^{-1} attributed to the characteristic absorption of eugenol (O-H) group [25-27]. The spectrum shows a peak at 675 cm^{-1} confirming the presence of the (Co-O) bond [28]. The (C=C) vibrations of the benzene ring was revealed at (1571, 1564, and 1419) cm^{-1}. The weak intensity band at 1234 cm^{-1} is assigned to the (C-O) vibration of eugenol [25-27].

The FTIR spectrum of [ZnO: Fe_2O_3/ Eug], **Figure 11** revealed a peak at 472 cm^{-1} that was assigned to stretching vibration of the (Zn-O) bond [24] and the broad absorption band at 3436 cm^{-1} attributed to the stretching vibration of eugenol (O-H) group [25-27]. The spectrum shows peaks at 543 cm^{-1}, confirming the presence of the (Fe-O) bond [29,30]. The (C=C) vibrations of benzene ring revealed at (1614, 1512, 1454, and 1407) cm^{-1}. The weak intensity band at 1290 cm^{-1} is assigned to (C-O) vibration of eugenol [25-27].

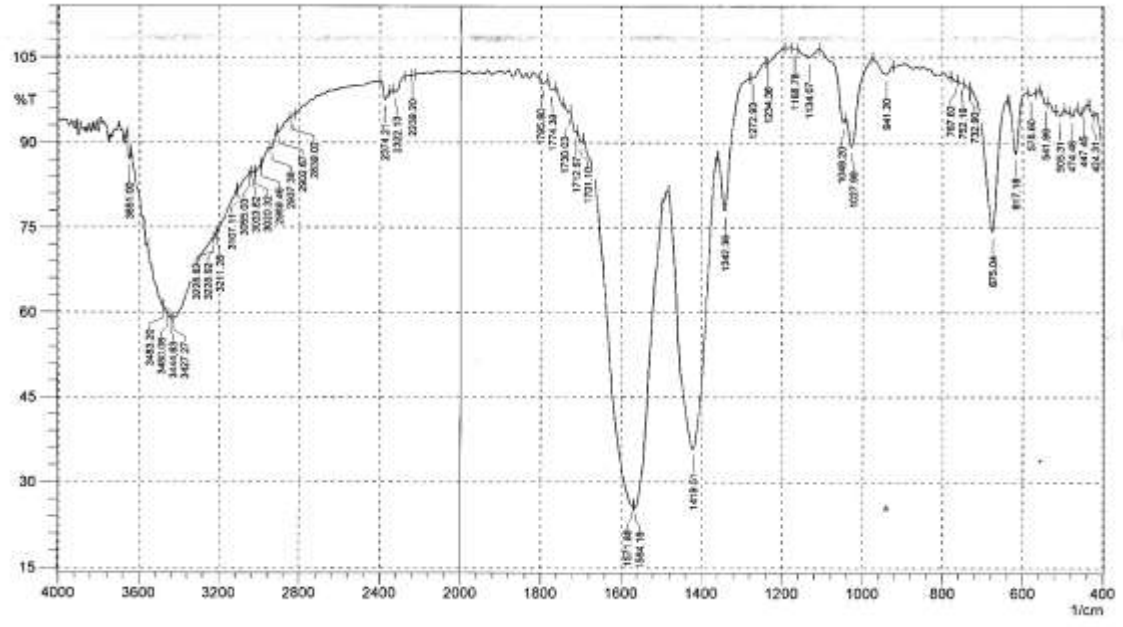

Figure 10. The FTIR spectrum of [ZnO: CoO/ Eug] nanocomposite

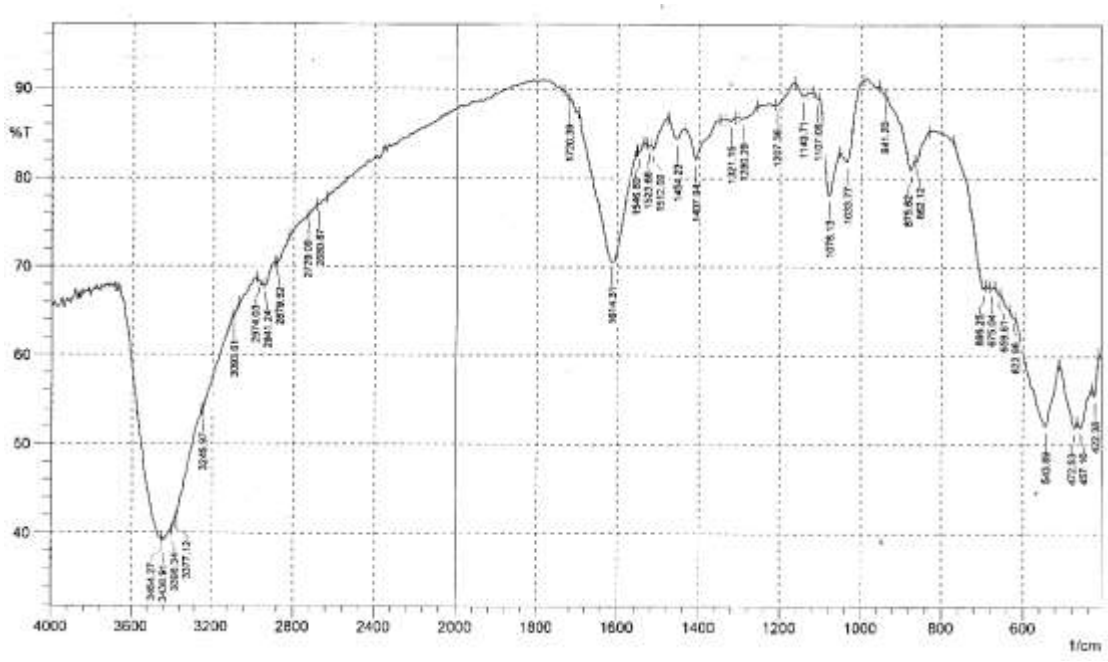

Figure 11. The FTIR spectrum of [ZnO: Fe_2O_3/ Eug] nanocomposite

3.5 Antimicrobial activity

The microbial activity of all synthesized nanostructures as nanocomposites was tested against two bacteria [*Escherichia Coli* (-) (*E. coli*), *Staphylococcus aureus* (+) (*S. aureus*)] and one fungi [*Candida albicaus* (C. *albicaus*)], it took (0.06 gm) from the cobalt, ferric oxides nanocomposites samples then, dissolved in 5 mL of dimethyl sulfoxide (DMSO), and the direct inhibitory effect of [nano metal oxides/ eugenol] against pathogenic microorganisms was determined by healthy diffusion method under aerobic condition [31], as shown in the Table 5. It has been observed that the levels of antibacterial and antifungal activities of [ZnO: CoO/ Eug] at the highest concentration of nanoparticles were the largest zone of inhibition (24 mm) against (*E. coil*) (27 mm) in (*S. aureus*) for bacteria and (37 mm) in (*C. albicaus*) for fungi. At the same time, the levels of antibacterial and antifungal activities of the [ZnO: Fe_2O_3/ Eug] were observed to be different in the inhibition zone, as shown in **Table 5**.

Table 5. Inhibition of pathogenic many bacteria and fungi on nanocomposites

Nanocomposites	E. coli (-) (mm)(bacteria)	S. aureus (+) (mm)(bacteria)	C. albicaus (mm)(fungi)
[ZnO: CoO/ Eug]	24	27	37
[ZnO: Fe_2O_3/ Eug]	16	20	22

3.6 Antioxidant activity

The biological activity of [ZnO: CoO/ Eug] and [ZnO: Fe_2O_3/ Eug] nanocomposites was tested by the DPPH method. (1,1-Diphenyl-2-picryl-hydroxyl) DPPH (4 mg) was dissolved in 100 ml of deionized water, and the solution was protected from light by covering the test tubes with aluminum foil. Various concentrations (100, 50, 25, 12.5, 6.25) ppm were prepared from compounds, where the first concentration was prepared by dissolving 1 mg of the compound and dissolving with 10 mL of methanol to be (100 ppm) and then diluted to be (50, 25, 12.5, 6.25)

ppm. The following equation was used to determine the potential to scavenge DPPH radicals, which is intensity (I) [32]:

I%= {(Abs blank – Abs sample) / Abs blank} x 100….. (1)

The absorbance of each solution was measured at 517 nm using a spectrophotometer after 1 hour of incubation at 37°C. Triplicates of all measurements were taken [32]. The results of nano compounds showed antioxidant activity against the DPPH free radical. They provided an excellent scavenging percentage, and the IC50 value of the synthetic compound was extracted, as shown in **Table 6**. In this project, we applied the antioxidant activity classification, which depends on IC50 range values published by Phongpaichit; the IC50 value was determined to assess the sample concentration required to inhibit 50% of the radical. The higher antioxidant activity = the lower (IC50) value, as shown in **Table 7**.

Table 6. Scavenging (%) for nanocompounds

Nanocomposite	Synthesized methods	Scavenging %					Linear eq.	R^2	Ic_{50}
		6.25 µg\ml	12.5 µg\ml	25 µg\ml	50 µg\ml	100 µg\ml			
[ZnO: Fe_2O_3/ Eug]	hydrothermal	42.8	48.2	53.2	55.8	81.3	y = 0.3819x + 41.463	0.9602	26.5
[ZnO: CoO/ Eug]	hydrothermal	41.3	43.2	47.7	51.1	73.5	y = 0.3346x + 38.396	0.969	34.7
Ascorbic acid	-	51.4	57.4	61.1	64.7	93.2	y = 0.4162x + 49.433	0.9572	1.4

Table 7. Antioxidant activity according to Phongpaichit

IC_{50} (µg/mL)	Mark antioxidant activity
10-50 µg/mL	Strong Antioxidant Activity
50-100 µg/mL	Intermediate Antioxidant Activity
>100 µg/mL	Weak Antioxidant Activity

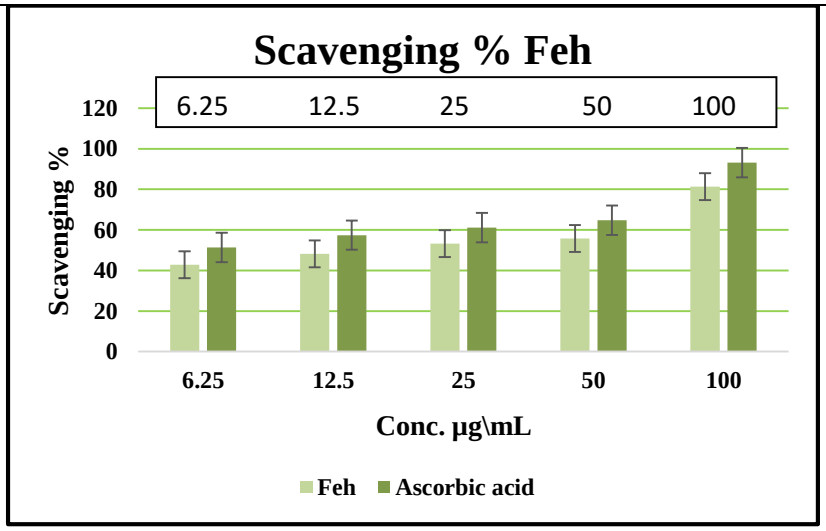

Figure 12. Antioxidant activity of [ZnO: Fe_2O_3/ Eug] nanocomposite

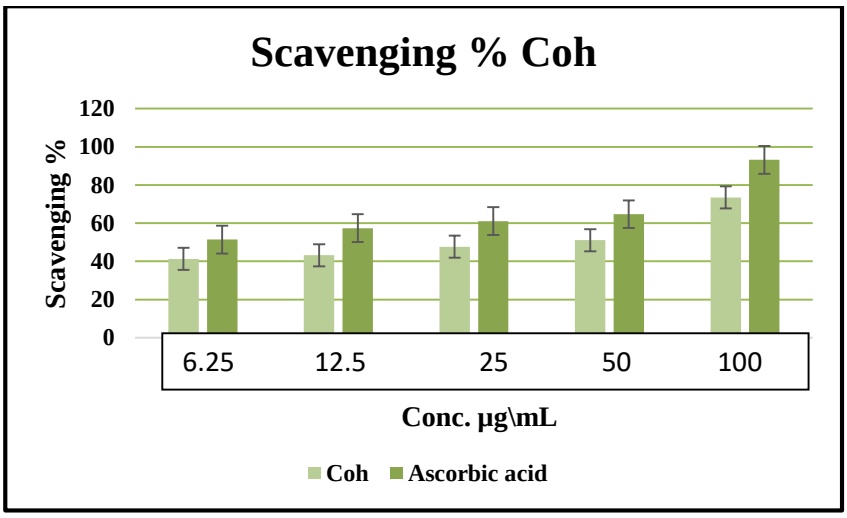

Figure 13. Antioxidant activity of [ZnO: CoO/ Eug] nanocomposite

4. Conclusion

The nanocomposites were synthesized by reacting eugenol with two metal oxides [zinc oxide (ZnO) and cobalt oxide (CoO)] to prepare the first compound [ZnO: CoO/ Eug] and [ZnO and Fe_2O_3 to prepare the second compound [ZnO: Fe_2O_3/ Eug] via the hydrothermal method. The measurements showed that the two composites were synthesized as a nanocomposites, where the nanoparticle's mean diameter is in the nanoscale range. Also, other measurements were made, including (FT-IR, SEM, EDX, and XRD). The effectiveness of the [ZnO: CoO/ Eug] and [ZnO: Fe_2O_3/ Eug] nanocomposites were tested on antibacterial and antifungal activity against two types of bacteria *[Escherichia Coli (-) (E. coli), Staphylococcus aureus (+) (S. aureus)]*, and kind of fungi *[Candida albicaus (C. abacus)]*, showed acceptable results and it has been observed that the levels of antibacterial and antifungal activities of [ZnO: CoO/ Eug] at the highest concentration of nanoparticles were the largest zone of inhibition comparison with [ZnO: Fe_2O_3/ Eug]. In addition, the antioxidant activity of the compounds against the free radical showed a good scavenging percentage.

Acknowledgment

The authors thank the Department of Chemistry/ College of Science/ University of Baghdad staff for their assistance in performing this research.

Conflict of Interest

The authors declare that they do not have any competing interests.

Funding

There is no financial support.

Ethical Clearance

This work has been approved by the Institutional Scientific Committee at the University of Baghdad/ College of Science.

References

1. Madkour, L.H. Introduction to nanotechnology (NT) and nanomaterials (NMs). *Nanoelectronic Materials*, **2019**, 1-47. Springer, Cham. http://dx.doi.org/10.1007/978-3-030-21621-4_1.
2. Atiya, M.A.; Hassan; A.K.; Kadhim, F.Q. Green synthesis of copper nanoparticles using tea leaves extract to remove Ciprofloxacin (CIP) from aqueous media. *IJS*, **2021**, *62*(*9*), 2833-2854. https://doi.org/10.24996/ijs.2021.62.9.1.
3. Komarneni, S. Feature article. Nanocomposites. *J. Mater. Chem*., **1992**, *12*(*2*), 1219-1230. https://doi.org/10.1039/JM9920201219.
4. Camargo, P.H.C.; Satyanarayana, K.G.; Wypych, F. Nanocomposites: synthesis, structure, properties and new application opportunities. *Mater. Res* **2009**, *12*, 1-39. http://dx.doi.org/10.1590/S1516-14392009000100002.
5. Farhan, R.Z.; Ebrahim, S.E. Preparing nanosilica particles from rice husk using precipitation method. *Baghdad Sci. J* **2021**, *18*(*3*), 494-500. https://doi.org/10.21123/bsj.2021.18.3.0494.
6. Zhang, H.; Chen, G. Potent antibacterial activities of Ag/TiO_2 nanocomposite powders synthesized by a one-pot sol− gel method. *Environ. Sci. Technol.* **2009**, *43*(*8*), 2905-2910. https://doi.org/10.1021/es803450f.
7. Abdulredha, S.T.; Abdulrahman, N.A. Cu-ZnO Nanostructures synthesis and characterization. *IJS*, **2021**, *62*(*3*),708-717. https://doi.org/10.24996/ijs.2021.62.3.1.
8. Hassan, E.; Al-saidi, M.H.; Rana, J.A.; Thahab, S.M. Preparation and characterization of ZnO nano-sheets prepared by different depositing methods. *IJS*, **2022**, *63*(*2*),538-547. https://doi.org/10.24996/ijs.2022.63.2.11.
9. Nisar, M.F.; Khadim, M.; Rafiq, M.; Chen, J.; Yang, Y.; Wan, C.C. Pharmacological properties and health benefits of eugenol: a comprehensive review. *Oxid Med Cell Longev* **2021**, *2021*, 2497354. https://doi: 10.1155/2021/2497354.
10. Thirukumaran, P.; Shakila, A.; Muthusamy, S. Synthesis and characterization of novel bio-based benzoxazines from eugenol. *Rsc Advances* **2014**, *16*(*4*), 7959-7966. https://doi.org/10.1039/C3RA46582A.
11. Aburel, O.M.; Pavel, I.Z.; Dănilă, M.D.; Lelcu, T.; Roi, A.; Lighezan, R.; Muntean, D.M.; Rusu, L.C. Pleiotropic Effects of Eugenol: The Good, the Bad, and the Unknown. *Oxid Med Cell Longev*., **2021**, 3165159. https://doi.org/10.1155/2021/3165159.
12. Nurdjannah, N.; Bermawie, N. Cloves. Handbook of Herbs and Spices. 2nd Edition. *Woodhead Publishing*, **2012**, *1*, 197-215. https://www.academia.edu/13434452/Handbook_of_herbs_and_spices_Volume_1_KV_Peter
13. Ulanowska, M.; Olas, B. Biological properties and prospects for the application of eugenol—A review. *Int. J. Mol. Sci*., **2021**, *22*(*7*), 3671. https://doi: 10.3390/ijms22073671.
14. Sethuram, L.; Thomas, J.; Mukherjee, A.; Chandrasekaran, N. Eugenol micro-emulsion reinforced with silver nanocomposite electrospun mats for wound dressing strategies. *Mater Adv*., **2021**, *2*(*9*), 2971-2988. https://doi.org/10.1039/D1MA00103E.
15. Thanh Chi, N.T.; Da, T.T.; Ha, N.V.; Dinh, N.H. Synthesis and spectral characterization of platinum (II) complexes containing eugenol, a natural allylphenol. *J Coord Chem*., **2017**, *70*(*6*), 1008-1019. http://dx.doi.org/10.1080/00958972.2017.1281917.
16. Zari, A.T.; Zari, T.A.; Hakeem, K.R. Anticancer properties of eugenol: A Review. *Molecules*, **2021**, *26*(*23*), 7407. https://doi.org/10.3390/molecules26237407.

17. Zhou, H.; Fu, W.; Muhammad, M.; Xie, M.; Xie, E.; Han, W. Self-assembled microspheres composed of porous ZnO/CoO nanosheets for aqueous hybrid supercapacitors. *J Phys D Appl Phys.*, **2019**, *52*(*50*), 505501. https://ui.adsabs.harvard.edu/link_gateway/2019JPhD...52X5501Z/doi:10.1088/1361-6463/ab4140.
18. Abid, M.A.; Abid, D.A.; Aziz, W.J.; Rashid, T.M. Iron oxide nanoparticles synthesized using garlic and onion peel extracts rapidly degrade methylene blue dye. *Physica B Condens Matter*, **2021**, *622*(*1*), 413277. http://dx.doi.org/10.1016/j.physb.2021.413277.
19. Wang, H.; Wang, M.; Tang, Y. A novel zinc-ion hybrid supercapacitor for long-life and low-cost energy storage applications. *Energy Storage Materials*, **2018**, *13*, 1-7. https://www.sciencedirect.com/science/article/pii/S240582971730644X.
20. Yousaf, S.A.; Ikram, M.; Ali, S. Significantly improved efficiency of organic solar cells incorporating Co_3O_4 NPs in the active layer. *Applied Nanoscience* **2018**, *8*(*3*), 489-497. https://ui.adsabs.harvard.edu/link_gateway/2018ApNan...8..489Y/doi:10.1007/s13204-018-0726-8.
21. Rashid, T.M.; Nayef, U.M.; Jabir, M.S.; Mutlak, F.A. Synthesis and characterization of Au: ZnO (core: shell) nanoparticles via laser ablation. *optik.*, **2021**, *244*(*24*), 167569. http://dx.doi.org/10.1016/j.ijleo.2021.167569.
22. Vinoth, V.; Subramaniyam, G.; Anandan, S.; Valdés, H.; Manidurai, P. Non-enzymatic glucose sensor and photocurrent performance of zinc oxide quantum dots supported multi-walled carbon nanotubes.*Mater. Sci. Eng.*, **2021**, *265*, 115036. https://doi.org/10.1016/j.mseb.2020.115036.
23. Gulina, L.; Tolstoy, V.; Kuklo, L.; Mikhailovskii, V.; Panchuk, V.; Semenov, V. Synthesis of Fe $(OH)_3$ microtubes at the gas–solution interface and their use for the fabrication of Fe_2O_3 and Fe microtubes. *Eur. J. Inorg. Chem.*, **2018**, *17*, 1842-1846. https://doi.org/10.1002/ejic.201800182.
24. Shamhari, N.M.; Wee, B.S.; Chin, S.F.; Kok, K.Y. Synthesis and characterization of zinc oxide nanoparticles with small particle size distribution. *Acta Chim Slov.*, **2018**, *65*(*3*), 578-585. http://dx.doi.org/10.17344/acsi.2018.4213.
25. Dhoot, G.; Auras, R.; Rubino, M.; Dolan, K.; Soto-Valdez, H. Determination of eugenol diffusion through LLDPE using FTIR-ATR flow cell and HPLC techniques. *Polymer*, **2009**, *50*(*6*), 1470-1482. https://doi.org/10.1016/j.polymer.2009.01.026.
26. Mahapatra, S.K.; Roy, S. Phytopharmacological approach of free radical scavenging and anti-oxidative potential of eugenol and Ocimum gratissimum Linn. *Asian Pac J Trop Biomed.*, **2014**, *7S1*, 391-397. https://doi.org/10.1016/s1995-7645(14)60264-9.
27. Matykiewicz, D.; Skórczewska, K. Characteristics and Application of Eugenol in the Production of Epoxy and Thermosetting Resin Composites: A Review. *Materials*, **2022**, *15*(*14*), 4824. https://doi.org/10.3390/ma15144824.
28. Govindasamy, R.; Raja, V.; Singh, S.; Govindarasu, M.; Sabura, S.; Rekha, K.; Rajeswari, V.D.; Alharthi, S.S.; Vaiyapuri, M.; Sudarmani, R.; Jesurani, S. Green synthesis and characterization of cobalt oxide nanoparticles using Psidium guajava leaves extracts and their photocatalytic and biological activities. *Molecules*, **2022**, *27*(*17*), 5646. https://doi.org/10.3390/molecules27175646.

29. Mohammadi, S.Z.; Khorasani-Motlagh, M.; Jahani, S.; Yousefi, M. Synthesis and characterization of α-Fe_2O_3 nanoparticles by microwave method. *Int J Biomed Nanosci Nanotechnol*., **2012**, *8*(*2*), 87-92. https://www.ijnnonline.net/article_3909.html.
30. Sankadiya, S.; Oswal, N.; Jain, P. and Gupta, N. Synthesis and characterization of Fe_2O_3 nanoparticles by simple precipitation method. *AIP Conf Proc*., **2016**, *1724*(*1*), 020064. https://doi.org/10.1063/1.4945184.
31. Abbey, T.C.; Deak, E. What's new from the CLSI subcommittee on antimicrobial susceptibility testing M100. *Clin Microbiol Newsl* **2019**, *41*(*23*), 203-209. https://doi.org/10.1016/j.clinmicnews.2019.11.002.
32. Maged, A.S.; Ahamed, L.S. Synthesis of new heterocyclic derivatives from 2-furyl methanethiol and study their applications. *Eurasian Chem. Commun*. **2021**, *3*, 461-476. https://doi: 10.22034/ecc.2021.279489.1158.